City Research Online

City, University of London Institutional Repository

Modelling and optimisation of design of non-conventional instrument transformers

Bojan Nikolić and Sanowar Khan

City, University of London, Northampton Square, London EC1V 0HB
United Kingdom

E-mail: bnikolic@ieee.org

Abstract. In this paper, we have proposed, modelled and optimised several designs of non-conventional instrument transformer (NCIT) for high voltage overhead transmission lines (400kV). We have discussed several parameters and investigated how they influence the sensitivity of our NCIT, consisting of magnetic shape memory (MSM) element, magnetic circuit and an LVDT (linear variable differential transformer). One of the most used conductors in these lines, 528-Al1/69-ST1A ACSR conductor (old code MOOSE), was modelled together with the MSM element and the magnetic circuit in ANSYS APDL. Based on the obtained results we have given suggestions on how NCIT could be designed taking into account a choice of the most appropriate material for this application. The way how the model was developed was presented as well as calculations of errors in the model in ANSYS APDL for electromagnetic problems.

1. Introduction

One of the main reasons that a need for so-called non-conventional instrument transformers (NCIT) has arisen recently is incompatibility of conventional instrument transformers with modern measurement equipment. Current and voltage transformers with an iron core are usually considered as conventional instrument transformers and their design has not changed significantly over the last few decades.

In our previous papers, we proposed a novel non-conventional instrument transformer based on magnetic shape memory (MSM) alloys for measuring electrical current in HV transmission lines and in this paper, that idea has been developed further [1, 2]. MSM alloys are relatively new materials which change their shape when subjected to external magnetic fields. The design of an NCIT, consisting of an MSM alloy element, a magnetic circuit and an LVDT, was optimised for 400kV high voltage overhead transmission lines. One of the most frequently used conductors in overhead transmission lines at high voltage level and above, 528-Al1/69-ST1A ACSR conductor (old code MOOSE), was modelled together with the MSM element and the magnetic circuit in ANSYS APDL [3, 4]. The model development was presented as well as calculations of discretisation error in ANSYS APDL for electromagnetic problems.

Our initial research showed that these sensors were not sensitive enough to be used in overhead transmission lines. By adding a magnetic circuit, in order to concentrate as much as possible magnetic field around the current-carrying conductor and focusing it towards the MSM element, this problem can be solved.

2. Designs of NCIT

A particular magnetic material called Hiperco 50 was proposed as a material for the magnetic circuit around the MSM element in our previous paper, taking into account several aspects, such as saturation flux density, resistivity, skin depth, availability in the market and others [2]. Since the skin depth of magnetic circuit is very small, a laminated magnetic circuit should be used.

The NCIT was modelled around the ACSR conductor 528-Al1/69-ST1A which consists of 54 aluminium strands and 7 steel strands in its core. Both, aluminium and steel strands, have equal diameters of d=3.53 mm. Similar models can be easily obtained for other types of conductors by slightly changing the code that we developed.

A 2D model of three different designs of the proposed NCIT can be seen in figure 1. The MSM element is placed between the poles. The dimensions of the MSM element that can be found in the market and are suitable for the proposed NCIT are 10 mm x 3 mm x 1 mm.

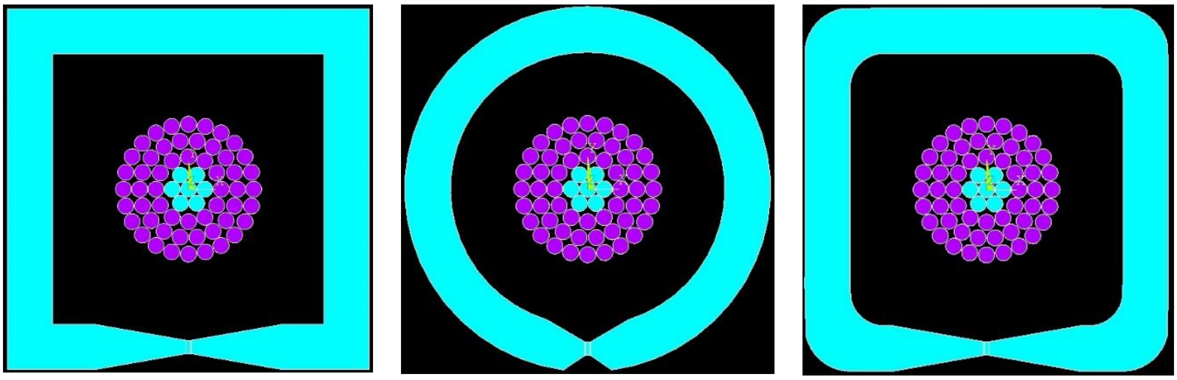

Figure 1. 2D model of the three different designs of the proposed NCIT around a 528-Al1/69-ST1A conductor – from left to right, rectangular, circular and rectangular magnetic circuit with rounded corners.

By analysing the strain-magnetic field relationship of MSM crystals (ETO Magnetic) at different pre-stress levels (loads) [5], it can be seen that the best option for our NCIT would be the MSM element which follows the 'ETO curve' at a load of 0.5 N/mm^2. This curve has the lowest threshold for triggering the MSM element (reversibly) and it has the largest strain. The MSM element would be triggered in this case by an approximately 0.085 T magnetic field, but higher values of the field are needed in order that the MSM element starts elongating linearly. MSM element consists of small parts called twin variants which start to reorient when magnetic field exceeds a certain threshold. This threshold is characterised by the minimum value of the external stress or magnetic field required to overcome the crystal's twinning stress and initiate reorientation. When an MSM element is not elongated it consists only of so-called hard variants. The relative magnetic permeability of MSM element in this situation is μ_r=2 what was used in this model. When the MSM element is fully elongated it consists of only so-called easy variants and its relative magnetic permeability is μ_r=50 in that case.

3. Optimisation of the magnetic circuit geometry

In order to optimise the magnetic circuit geometry for the application of NCIT for high voltage overhead transmission lines, we have analysed several parameters: size of the airgap (the airgap between the MSM element and the poles), position of the magnetic circuit relative to the conductor (distance between the centre of the conductor and the inner side of the magnetic circuit, r), magnetic circuit's width w and the distance from the airgap to the point where the poles start to taper, t. Comparisons have been done for the rectangular Hiperco 50 magnetic circuit.

Table 1 shows the variation of magnetic field amplitude on the surface of the MSM element, B_{surface}, and the maximum value of magnetic field inside the magnetic circuit, $B_{\max}$, when the size of the airgap has been changed while keeping the other parameters constant.

Table 1. Variation of magnetic flux density on the surface of the MSM element and in the magnetic circuit with the airgap (Current *I*=500 A, *f*=50 Hz).

w [mm]	*t* [mm]	*r* [mm]	*w* [mm]	Bsurface [T]	Bsurface [%]	Bmax in mag. circuit [T]	Bmax in mag. circuit [%]
10	20	30	10	0.33	0	2.213	0
10	20	30	10	0.306	-7.27	2.195	-0.81
10	20	30	10	0.285	-13.64	2.179	-1.54

It can be seen that even a small increase in the airgap significantly decreases the magnetic flux density on the surface of the MSM element. In order to increase the sensitivity of the NCIT, it is better that its size is as small as possible. As the further decrease in the airgap is limited by technological factors, the best choice for the airgap was found to be 0.1 mm.

As discussed in [2], we modelled the 528-Al1/69-ST1A ACSR conductor (old code MOOSE). The overall diameter of this conductor is 31.8 mm which means that the magnetic circuit around the conductor can be placed only in a way that r>15.9 mm. The magnetic circuit geometry should be carefully chosen as it affects its saturation, NCIT's sensitivity to high temperatures of the conductor and, finally, possibility to trigger the MSM element.

Table 2 shows the variation of magnetic flux densities Bsurface and Bmax, with the position of the magnetic circuit relative to the conductor.

Table 2. Variation of magnetic flux density on the surface of the MSM element and in the magnetic circuit with distance, *r* between the conductor and the magnetic circuit (*I*=500 A, *f*=50 Hz).

w [mm]	*t* [mm]	*r* [mm]	Bsurface[T]	Bsurface[%]	Bmax in mag. circuit [T]	Bmax in mag. circuit [%]
10	20	25	0.354	100.00	2.357	100.00
10	20	30	0.33	-6.78	2.213	-6.11
10	20	40	0.293	-17.23	2.091	-11.29
10	20	50	0.264	-25.42	1.987	-15.70
10	20	60	0.241	-31.92	1.849	-21.55

Since the flux density on the surface of the MSM element decreases significantly as the magnetic circuit is placed away from conductor, it should be placed as close as possible to the conductor, but yet far enough so that the heat around conductor does not affect the magnetic circuit and the temperature-sensitive MSM element. A distance of r=25-30 mm could be a solution.

Tables 3 and 4 show the change of Bsurface and Bmax, when the width of the magnetic circuit, *w* and the above geometric parameter of the poles, *t* have been changed.

There needs to be trade-off with respect of the width, *w*. A narrow magnetic circuit, although more sensitive, saturates more easily. On the other hand, a wide magnetic circuit is not very practical as it will increase the size of the NCIT as well as its cost. We have found that a w=10 mm magnetic circuit is a reasonable trade-off.

From table 4, it can be seen that tapering of poles does not affect significantly the magnetic flux density on the MSM surface, but still it increases. Thus, it is recommended to taper pole ends as much as its geometry allows. For example, for r=30 mm, this value could be chosen around t=20 mm.

Finally, we have compared sensitivity of all three NCIT's designs in figure 1 for similar geometric parameters. Results are shown in table 5.

As expected, the rounding of corners of rectangular magnetic circuit has improved the sensitivity of the NCIT ($B_{surface}$ is comparable to that of the circular design). Although any of the three proposed designs can be used, due to practical reasons of handling and mounting of the NCIT around the conductor, the preferred design would be the rectangular one with rounded corners.

Table 3. Variation of magnetic flux density on the surface of the MSM element and in the magnetic circuit with the width, *w* of the magnetic circuit (*I*=500 A, *f*=50 Hz).

w [mm]	*t* [mm]	*r* [mm]	$B_{surface}$ [T]	$B_{surface}$ [%]	B_{max} in mag. circuit [T]	B_{max} in mag. circuit [%]
5	20	30	0.338	0	2.31	0
8	20	30	0.333	-1.48	2.213	-4.20
10	20	30	0.33	-2.37	2.213	-4.20
15	20	30	0.321	-5.03	2.231	-3.42
20	20	30	0.312	-7.69	2.217	-4.03
25	20	30	0.302	-10.65	2.227	-3.59

Table 4. Variation of magnetic flux density on the surface of the MSM element and in the magnetic circuit with the distance, *t*, (*I*=500 A, *f*=50 Hz).

w [mm]	*t* [mm]	*r* [mm]	$B_{surface}$[T]	$B_{surface}$ [%]	B_{max} in mag. circuit [T]	B_{max} in mag. circuit [%]
10	10	30	0.322	0	2.231	0
10	15	30	0.327	1.55	2.245	0.63
10	20	30	0.33	2.48	2.213	-0.81

Table 5. Magnetic flux density on the surface of the MSM element and in the magnetic circuit for three different magnetic circuit designs of NCIT (I=400 A, f=50 Hz).

Shape of magnetic circuit	*w* [mm]	*t* [mm]	*r* [mm]	$B_{surface}$ [T]	$B_{surface}$ [%]	B_{max} in mag. circuit [T]	B_{max} in mag. circuit [%]
Circular	10	20	40	0.237	0	1.9981	0
Rectangular	10	20	40	0.224	-5.49	1.8926	-5.28
Rectangular with rounded corners	10	20	40	0.23	-2.95	2.047	2.45

4. Model development and errors in the model

The model of the conductor, MSM element and magnetic circuit was developed in ANSYS APDL. It consists of 5 different materials (aluminium, steel, air, Hiperco50 and MSM alloy). The element Plane53 was used for modelling. This is an eight nodes element which is based on the magnetic vector potential formulation and has a nonlinear magnetic capability for modelling B-H curves.

The mesh was obtained using ANSYS's Mesh Tool where the level of fineness can be set between 1 (the finest mesh) and 10 (the roughest mesh). Additional refinements were required, especially in the most sensitive areas such as in magnetic circuit and in the air gap between the MSM element and the magnetic circuit's poles. The level of refinement can be chosen in the range from 1 to 5. The choice of level 1 means that the selected part of mesh will be the least refined while by choosing the level 5 the most new elements will be added.

In an electromagnetic analysis, ANSYS APDL allows calculating the mesh discretisation error for the parts of the model using macro EMAGERR. Two parameters are used to describe its value: B_{ei} - relative error for the magnetic flux density (magnitude) for element *i* and its normalised value, B_{nei}. They can be calculated using the equations (4.1) and (4.2), respectively.

$$B_{ei} = \frac{1}{n}\sum_{j=1}^{n}\left|B_j - B_{ij}\right| \tag{4.1}$$

where:

B_j - nodal averaged magnetic flux density (magnitude),
B_{ij} - magnetic flux density (magnitude) of element i at node j

$$B_{nei} = \frac{B_{ei}}{B_{max}} \tag{4.2}$$

where:
B_{max} - maximum nodal averaged magnetic flux density (magnitude)

The airgap between the MSM element and the poles of the magnetic circuit is the most delicate part of the model due to its geometry and presence of several different materials, and at the same time, the one which is of the particular interest for obtaining the simulation results. Therefore, B_{ei} and B_{nei} errors were calculated specifically for that part of the model.

The calculation is valid within a material boundary and does not consider the error in continuity of fields across dissimilar materials. Therefore, in addition to the values of B_{ei} and B_{nei}, in order to control the error in the model, it is required to check the values of the normal component of B on the border between two materials (air in the airgap and Hiperco 50 in the magnetic circuit). Ideally, there should be no difference in their values, but in FEM simulations that never happens. It is convenient to observe the relative error due to this discontinuity which is given by equation (4.3):

$$B_{nerr}\,[\%] = \frac{B_{nair} - B_{nmag}}{B_{nair}} \cdot 100 \tag{4.3}$$

where:
B_{nair} – normal component of B in the airgap on the border with the magnetic circuit,
B_{nmag} – normal component of B in the magnetic circuit on the border with the airgap

The values of the above-mentioned parameters will obviously depend on the chosen geometry, mesh fineness, loads, and so on. Several models with different levels of mesh fineness were developed and tested.

Figure 2 shows a mesh of one of the suggested designs – a rectangular magnetic circuit with rounded corners (w=10 mm, t= 20 mm, r=30 mm, I=500 A) as well as the mesh of the part including the MSM element, the airgaps around it and the poles of the magnetic circuit.

The maximum value of B_{nei} for the observed part was $B_{nei\,(max)}$=0.06832 and discontinuity on the border was B_{nerr}=0.63 %. The total number of elements in the model was 329,794 out of which 121,299 were in the airgap between the MSM element and the pole of the magnetic circuit. This mesh was chosen due to its precision of obtained results and yet still not a long time to obtain results on the computer that was used for simulations. Increasing the number of elements in the model particularly affects the value of B_{nerr}. As an example, it can be mentioned that this parameter took values from 17.15 % for the mesh consisting of 13,486 elements (136 elements in the airgap) to 0.63 % for the presented case. At the same time, the range of B_{nei} was 0.033-0.093. The number of elements in the presented model is relatively high, but it is worth it to mention that, for example, B_{nerr}=1.96 % was achieved with 47,424 elements out of which 14,561 were in the airgap. Furthermore, it should be said that a convergence tolerance in the model was 0.001.

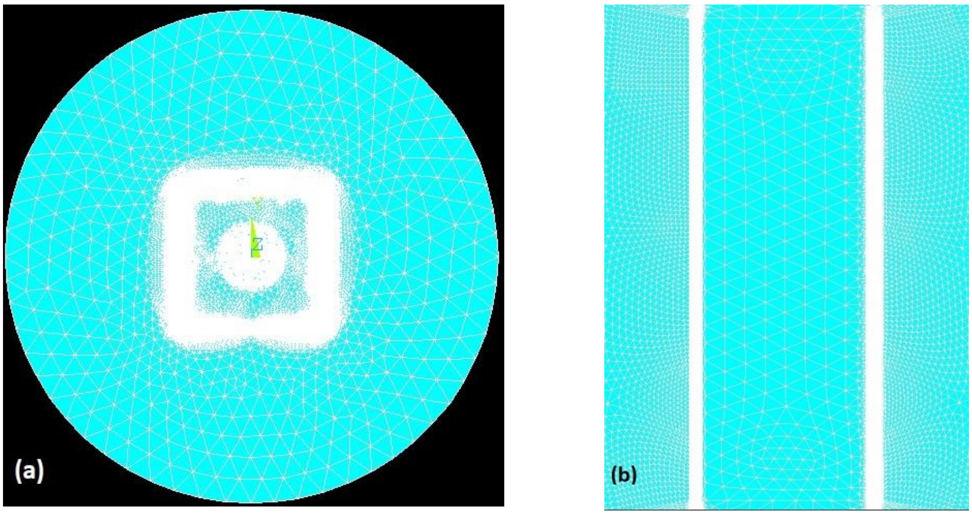

Figure 2. Mesh of one of the suggested designs – a rectangular magnetic circuit with rounded corners (*w*=10mm, *t*=20mm, *r*=30mm) a) full model b) MSM element, airgaps and poles of magnetic circuits.

5. Conclusions

In this paper, we have analysed parameters that affect the sensitivity of the proposed NCIT designs in order to optimise its magnetic circuit geometry for high voltage overhead transmission lines (400kV). One of the most used conductors in these lines, the 528-Al1/69-ST1A ACSR conductor, was modelled together with the MSM element and the magnetic circuit in ANSYS APDL.

We have proposed and modelled three designs of magnetic circuit and presented how variation of different parameters (e.g. airgap size, placement of magnetic circuit in relation to the conductor, and its various dimensions) affect, for example magnetic flux density on the surface of the MSM element and in the magnetic circuit.

The way how the model was developed was shown as well as calculations of errors in the model in ANSYS APDL for electromagnetic problems. The obtained results for one of the suggested designs were presented.

Based on the results obtained so far, we have recommendations on NCIT design taking into account a choice of the most appropriate material for this application. Before a viable prototype can be designed, more NCIT modelling and analyses of other parameters will be done in our future work.

6. References

[1] Nikolić B, Khan S and Gabdullin N 2016 Development of non-conventional instrument transformers (NCIT) using smart materials *J. Phys.: Conf. Ser.* **772** 012065

[2] Nikolić B and Khan S 2018 Modelling of non-conventional instrument transformers (NCIT) by FEM *J. Phys. Conf.: Ser.* **1065** 072046

[3] British Standards Institution 2013 BS EN 50182:2001 Conductors for Overhead Lines - Round Wire Concentric Lay Stranded Conductors (London, England: BSI) pp 27-74

[4] Lings R 2005 Overview of transmission lines above 700 kV *IEEE Power Engineering Society Inaugural Conference and Exposition in Africa*, 2005 pp 11–15.

[5] EtoMagnetic: Magnetic Shape Memory Technology (MAGNETOSHAPE) http://etogroup.com/MAGNETOSHAPE_EN.html